ORIGINAL RESEARCH

Long-Term Outcome of Additional Superior Vena Cava to Septal Linear Ablation in Catheter Ablation of Atrial Fibrillation

Moo-Nyun Jin, MD;* Byounghyun Lim, PhD;* Hee Tae Yu, MD, PhD; Tae-Hoon Kim, MD; Jae-Sun Uhm, MD, PhD; Boyoung Joung, MD, PhD; Moon-Hyoung Lee, MD, PhD; Chun Hwang, MD; Hui-Nam Pak, MD, PhD

Background—We previously reported the benefit of linear ablation from the superior vena cava to the right atrial septum (SVC-L) within a year after circumferential pulmonary vein isolation (CPVI) in patients with paroxysmal atrial fibrillation (AF). We explored the long-term effects of SVC-L and its potential related mechanisms.

Methods and Results—Among 2140 consecutive patients with AF ablation, we included 614 patients (73.3% male, aged 57.8±10.7 years, 13.7% with persistent AF) who did not undergo an extra–pulmonary vein left atrial ablation after propensity score matching; of those, 307 had additional SVC-L and 307 had CPVI alone. We evaluated the heart rate variability and computational modeling study to explore mechanisms. Although the procedure time was longer in the SVC-L group than the CPVI group ($P<0.001$), the complication rates did not differ ($P=0.560$). During 40.5±24.4 months of follow-up, the rhythm outcome was significantly better in the SVC-L group than the CPVI group (log rank, $P<0.001$). At 2-year follow-up of heart rate variability, a significantly higher mean heart rate ($P=0.018$) and a lower ratio of low/high-frequency components ($P=0.011$) were found with SVC-L than CPVI alone. In realistic in silico biatrial modeling, which reflected the electroanatomies of 10 patients, SVC-L significantly reduced biatrial dominant frequency compared with CPVI alone ($P<0.001$) and increased AF termination and defragmentation rates ($P=0.033$).

Conclusions—SVC-L ablation in addition to CPVI significantly improved the long-term rhythm outcome over 2 years after AF catheter ablation by mechanisms involving autonomic modulation and AF organization. **(*J Am Heart Assoc*. 2019;8:e013985. DOI: 10.1161/JAHA.119.013985.)**

Key Words: atrial fibrillation • catheter ablation • recurrence • superior vena cava

Since Coumel et al[1] reported that the cardiac autonomic nervous system (ANS) activity contributes to the initiation of paroxysmal atrial fibrillation (AF), many studies have been conducted to prove the role of the cardiac ANS in the initiation and maintenance mechanisms of AF.[2–4] Ganglionated plexi (GPs), a part of the typical intrinsic cardiac ANS, are buried in epicardial fat pads near the junction of the left atrium (LA) and the pulmonary vein (PV), and complex neural trafficking is achieved through these autonomic nerve plexi.[5,6] In an effective AF rhythm control strategy, catheter ablation involving a long-lasting circumferential PV isolation (CPVI) is known to be the most important factor, and a transmural wide CPVI is known to have a partial denervation effect on the GPs located in the epicardial aspect of the LA–PV junction.[7] However, it is known that a selective GP ablation without a CPVI is not adequate to achieve an anti-AF effect, and the effect of a surgical GP ablation in patients with persistent AF with atrial remodeling is controversial.[8,9] The third fat pad, which comprises the gatekeeper ganglia of typical extrinsic cardiac vagal nerves, is located at the junction of the superior vena cava (SVC) and aorta.[10] Kang et al[11] reported improved attenuation of heart rate variability (HRV) and 1-year rhythm outcome after linear ablation from the SVC to the right atrial septum (SVC-L), crossing the third fat pad area, in addition to conventional CPVI. Debruyne et al[12] reported improvement in neutrally mediated syncope and functional sinus node dysfunction by ablation of the SVC–septal area corresponding to the anterior right GPs. However, the long-term changes in autonomic neural function and the long-term recurrence rate after additional SVC-L during the AF ablation procedure are

From the Division of Cardiology, Yonsei University Health System, Seoul, Republic of Korea (M.-N.J., B.L., H.T.Y., T.-H.K., J.-S.U., B.J., M.-H.L., H.-N.P.); Utah Valley Medical Center, Provo, UT (C.H.).

Accompanying Tables S1 through S3 and Figures S1 through S4 are available at https://www.ahajournals.org/doi/suppl/10.1161/JAHA.119.013985

*Dr Jin and Dr Lim contributed equally to this work.

Correspondence to: Hui-Nam Pak, MD, PhD, 50 Yonseiro, Seodaemun-gu, Seoul, Republic of Korea 120-752. E-mail: hnpak@yuhs.ac

Received July 17, 2019; accepted October 23, 2019.

Clinical Perspective

What Is New?

- Linear ablation from the superior vena cava to the septum in addition to circumferential pulmonary vein isolation improves the long-term rhythm outcome of catheter ablation for atrial fibrillation.
- Linear ablation from the superior vena cava to the right atrial septum results in long-term vagal denervation effects reflected by heart rate variability 2 years after atrial fibrillation ablation.
- Additional linear ablation from the superior vena cava to the right atrial septum reduces biatrial dominant frequency evaluated by computational modeling study.

What Are the Clinical Implications?

- Linear ablation from the superior vena cava to the septum in addition to pulmonary vein isolation can be considered in catheter ablation of atrial fibrillation.

unknown. The aim of this study was to evaluate the efficacy and mechanisms of SVC-L in AF patients who did not undergo an extra-PV LA ablation during the AF ablation procedure and who had their HRV followed for >2 years. We assessed the cardiac ANS function based on the HRV analysis and AF wave dynamics using a realistic biatrial simulation modeling study after SVC-L.

Methods

Anonymized data, materials, and analytic methods will be made available to other researchers for reasonable purposes of reproducing the results or replicating the procedure.

Study Population

This study protocol adhered to the principles of the Declaration of Helsinki and was approved by the institutional review board of the Yonsei University Health System. All patients provided written informed consent for inclusion in the Yonsei AF Ablation Cohort Database (ClinicalTrials.gov identifier: NCT02138695). Between March 2009 and December 2016, we screened 2140 consecutive patients in the Yonsei AF Ablation Cohort Database who underwent radiofrequency catheter ablation (RFCA). Patients were categorized into 2 groups according to the RFCA method: CPVI alone (CPVI group) and CPVI plus SVC-L (SVC-L group). Exclusion criteria for the study were as follows: (1) AF with rheumatic valvular disease, (2) structural heart disease other than left ventricular hypertrophy, (3) history of prior RFCA, (4) history of cardiac surgery, (5) additional linear ablation in the LA, (6) additional ablation of complex fractionated electrograms, and (7) follow-up period of <2 years after the procedure. Among 2140 registered patients, 822 who did not undergo an extra-PV LA ablation were included in this study: 347 with CPVI alone and 475 with CPVI plus SVC-L. After 1:1 propensity score matching, 614 patients were finally analyzed, with 307 patients in each group. Figure 1 shows the patient flowchart of this study.

All patients were imaged using 3-dimensional (3D) spiral computed tomography (CT; Philips Brilliance 64, 64-channel, lightspeed volume CT) to visually define the anatomy of the LA and PVs. All patients received oral anticoagulation therapy with vitamin K antagonists or non–vitamin K oral anticoagulants at least 1 month before and 3 months after the procedure. All antiarrhythmic drugs (AADs) were discontinued for at least 5 half-lives, and amiodarone was stopped at least 4 weeks before the procedure.

Electrophysiologic Mapping

An electrophysiology study was performed using a decapolar catheter (Bard Electrophysiology) in the high right atrium (RA), a duo-decapolar catheter (St. Jude Medical Inc) in the low RA and inside the coronary sinus, and a quadripolar catheter in the SVC recording region. Intracardiac electrograms were recorded using the Prucka CardioLab Electrophysiology system (GE Medical Systems), and RFCA was performed in all patients using 3D electroanatomical mapping (NavX [St. Jude Medical] or CARTO [Biosense Webster]) merged with 3D spiral CT. Double transseptal punctures were made, and multiview pulmonary venograms were obtained. Systemic anticoagulation was performed with intravenous heparin to maintain an activated clotting time of 350 to 400 seconds during the procedure. For electroanatomical mapping, the 3D geometry of both the LA and the PV was generated using 3D electroanatomical mapping systems and then merged with the 3D spiral CT images.

Radiofrequency Catheter Ablation

The details of the RFCA technique and strategy were described in our previous studies.[11] Briefly, for CPVI ablation, continuous circumferential lesions were created at the level of the LA antrum encircling the right and left PVs using an open-irrigated, 3.5-mm–tip deflectable catheter (25–35 W, 45°C; Celsius and Smart-Touch [Johnson & Johnson] or Coolflex [St. Jude Medical];). The end point of the CPVI was the electric isolation of the PV potentials and bidirectional block of the PVs. The CPVI was verified during an isoproterenol infusion after a waiting time of 30 minutes. All patients underwent a cavotricuspid isthmus ablation with an end point of bidirectional conduction block. SVC-L ablation started from the

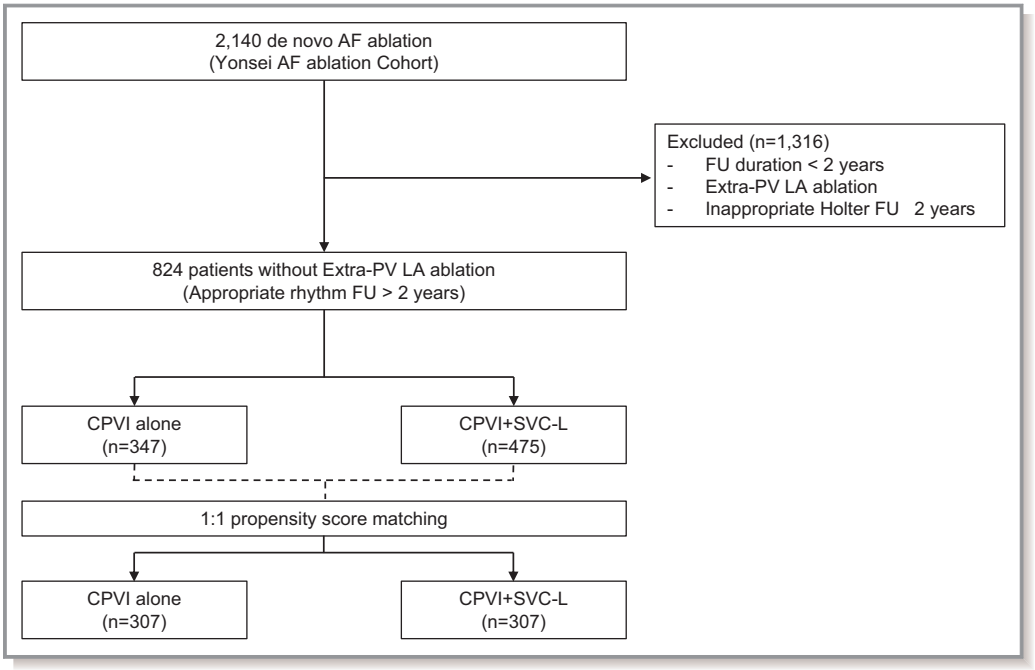

Figure 1. Flowchart of group distribution of the study. AF indicates atrial fibrillation; CPVI, circumferential pulmonary vein isolation; FU, follow-up; LA, left atrium; PV, pulmonary vein; SVC-L, linear ablation from the superior vena cava to the right atrial septum.

highest septal aspect of SVC while monitoring the reduction in voltage amplitude and elimination of sharp potentials along the SVC-L (30 W, 20-second ablation at each point, 10–40 g of catheter contact force). The tip of the catheter was directed toward the septal side guided by the left and right anterior oblique 35° views and a 3D electroanatomical map (Figure S1). At the SVC–RA junction, we extended the linear ablation lesion to the upper posterior limbus of the fossa ovalis.

Holter Monitor Recordings and HRV Analysis

The HRV was analyzed by 24-hour Holter monitor recordings taken in each patient during the pre- and postablation periods at 3, 12, and 24 months with a GE Marquette MARS 8000 Holter analyzer (GE Medical Systems). After identifying each QRS complex, the numerical series of RR intervals were calculated. Only high-quality recordings were considered for analysis. All recordings were digitized and reviewed by an experienced operator. Premature ventricular beats, premature atrial beats, and electrical artifact were excluded from the analysis. The HRV parameters were used as indicators of the autonomic activity according to the previously published guidelines. The mean heart rate and following time–domain HRV parameters were analyzed: mean RR interval (mean NN interval), standard deviation of the NN intervals, standard deviation of the 5-minute means of the NN intervals, and root mean square of successive differences between NN intervals. The following parameters were calculated: very low-frequency components (0.040 Hz), low-frequency components (LF; 0.040–0.150 Hz), high-frequency components (HF; 0.150–0.400 Hz), and the LF/HF ratio. HF and root mean square of successive differences were indicators of the parasympathetic nervous activity, and LF and LF/HF ratio reflected the sympathetic nervous activity and sympathovagal balance, respectively.

Postablation Management and Follow-Up

The patients visited the outpatient clinic regularly at 1, 3, 6, and 12 months and then every 6 months thereafter or whenever symptoms occurred after the RFCA. All patients underwent ECG recordings at every visit and 24-hour Holter recordings at 3 and 6 months and every 6 months, according to the 2012 Heart Rhythm Society/European Heart Rhythm Association/European Cardiac Arrhythmia Society Expert Consensus Statement guidelines. Holter monitoring or event-monitor recordings were obtained when patients reported symptoms of palpitations suggestive of an arrhythmia recurrence. Holter analysis and adjudication were performed by an individual blinded to the study group assignment. AF recurrence was defined as any episode of AF or atrial tachycardia of at least 30 seconds in duration. Any ECG documentation of an AF recurrence within a 3-month blanking period was diagnosed as an early recurrence, and an AF recurrence >3 months after the procedure was diagnosed

as a clinical recurrence. The primary study end point was freedom from documented episodes of AF or atrial tachycardia lasting >30 seconds and occurring after a 3-month blanking period after a single ablation procedure, with or without the use of AADs.

Computer Simulation of Biatrial Modeling

We evaluated the effect of the SVC-L on the AF wave dynamics in a realistic biatrial computational model reflecting the patient's atrial anatomy and electrophysiology in a retrospective manner. We integrated the 3D structures of the atria obtained from the patients' CT images and voltage and local activation electrograms acquired by the EnSite NavX system (Endocardial Solutions; Abbott) for a computational modeling simulation. The modeling study included a total of 10 paroxysmal AF patients (9 men; mean age: 64.9±10.1 years) whose electroanatomical bipolar electrogram data were integrated (NavX system). A mesh was generated and refined by CUVIA software (model SH01, v2.5; Laonmed) with a triangular type.[13] Each triangular mesh consisted of 3 nodes, and between 600 000 and 850 000 nodes were generated in the model. Cellular ionic currents were calculated based on the Courtemanche human atrial model.[14] Ramp pacing stimulation was started near the PV area, and pacing stimuli were performed with cycle lengths of 200, 190, and 180 ms. The overall pacing duration was 4560 ms. We measured the dominant frequency values for 6 seconds after AF induction. A virtual ablation was conducted by generating conduction blocks at CPVI or SVC-L, and the AF termination and defragmentation rates were determined within 60 seconds after the virtual intervention.

Statistical Analysis

Continuous variables are expressed as mean±SD, and categorical variables are expressed as frequency (percentage). Normality tests were performed for each variable to determine whether a data set was well modeled by a normal distribution. Continuous variables were compared by Student *t* tests or a Mann–Whitney *U* test, whereas categorical variables were compared using a χ^2 test or Fisher exact test. To compare the serial changes in the HRV parameters over time, we used a linear mixed-model analysis. A multivariable Cox proportional hazards regression analysis was used to identify any predictors associated with AF recurrence. A Kaplan–Meier analysis with a log-rank test was used to calculate AF recurrence–free survival over time and to compare the recurrence rates across groups. To reduce any selection bias for the treatment and any other related potential confounding factors in the observation study, we performed a baseline characteristic adjustment for the patients using propensity scores. Propensity scores were estimated using a nonparsimonious multiple logistic regression model for the SVC-L and CPVI-alone groups. The following variables were entered: age, sex, type of AF, comorbidities, and AAD and β-blocker use after ablation. Pairs were matched 1:1 by an optimal balance, without a replacement. A matching caliper of 0.1 SD of the logic of the estimated propensity score was enforced to ensure that matches of poor fit were excluded. A 2-sided $P<0.05$ was considered to indicate statistical significance. The statistical analyses were performed using SPSS v23.0 (IBM Corp) and R v3.4.4 (R Foundation for Statistical Computing) software.

Results

Patient Characteristics and Procedural Results

We compared 307 patients in the CPVI group and 307 in the SVC-L group (Figure 1). There was no significant difference between groups in terms of age, sex, proportions of persistent AF, hypertension, diabetes mellitus, heart failure, previous strokes, and follow-up duration; propensity score matching yielded a cohort that was well balanced for all baseline covariates (Table 1). The procedural results are summarized in Table 2. The procedure time ($P<0.001$) and ablation time ($P<0.001$) were significantly longer in the SVC-L group than the CPVI group, but the procedure-related complication rates did not differ between groups.

Long-Term Clinical Outcomes

During 40.5±24.4 months of follow-up, both the early recurrence rate (24.4% versus 32.6%, $P=0.025$) and the clinical recurrence rate (26.1% versus 46.3%, $P<0.001$) were significantly lower in the SVC-L group than the CPVI group (Table 2). Kaplan–Meier analysis also showed a superior rhythm outcome in the SVC-L group compared with the CPVI group in the matched patients (log rank, $P<0.001$; Figure 2A), and AAD-free AF recurrence was also significantly lower in the SVC-L group than the CPVI group (Log-rank, $P<0.001$ Figure 2B). The AAD prescription rates at discharge did not differ between groups (5.5% versus 5.5%, $P=1.000$). However, we prescribed AADs in patients with early recurrence within 3 months, and the SVC-L group had less AAD use than the CPVI alone group after 3 months of treatment (15.3% versus 21.8%, $P=0.038$; Table 2). Among 222 patients (36.2%) with clinical recurrence, the proportions of atrial tachycardia (28.7% [23/80] versus 32.4% [47/142], $P=0.573$) and that requiring cardioversion (16.3% [13/80] versus 17.6% [25/142], $P=0.797$) did not significantly differ between groups (Table 2). Overall, 4.2% (13/307) of the SVC-L group and 8.1% (25/307) of the CPVI group underwent cardioversion to

Table 1. Baseline Characteristics of the Total and PS-Matched Populations

	Total Population			PS-Matched (1:1) Population			
	SVC-L Group (n=475)	CPVI Group (n=347)	*P* Value	Overall After PS Match (n=614)	SVC-L Group (n=307)	CPVI Group (n=307)	*P* Value
Age, y	60.2±11.2	56.9±11.1	<0.001	57.8±10.7	57.9±10.7	57.7±10.7	0.178
Male, %	319 (67.2)	258 (74.4)	0.026	450 (73.3)	225 (73.3)	225 (73.3)	1.000
Body mass index, kg/m^2	24.7±3.1	24.7±2.7	0.850	24.8±3.0	24.9±3.2	24.7±2.8	0.614
Paroxysmal AF (%)	379 (79.8)	305 (87.9)	0.002	530 (86.3)	265 (86.3)	265 (86.3)	1.000
Comorbidities							
Heart failure (%)	46 (9.7)	15 (4.3)	0.004	32 (5.2)	17 (5.5)	15 (4.9)	0.716
Hypertension (%)	233 (49.1)	141 (40.6)	0.017	270 (44.0)	138 (45.0)	132 (43.0)	0.626
Diabetes mellitus (%)	88 (18.5)	32 (9.2)	<0.001	62 (10.1)	30 (9.8)	32 (10.4)	0.789
Stroke/TIA (%)	64 (13.5)	24 (6.9)	0.003	49 (8.0)	25 (8.1)	24 (7.8)	0.882
Vascular disease (%)	95 (20.0)	34 (9.8)	<0.001	69 (11.2)	37 (12.1)	32 (10.4)	0.523
Chronic kidney disease (%)	52 (10.9)	32 (9.2)	0.422	56 (9.1)	30 (9.8)	26 (8.5)	0.566
CHA_2DS_2-VASc score	2.1±1.7	1.3±1.3	<0.001	1.5±1.4	1.5±1.4	1.4±1.3	0.146
Echocardiography							
LA dimension, mm	40.1±5.9	39.8±6.0	0.450	39.9±5.9	39.7±5.7	40.0±6.1	0.661
LA volume index, mL/m^2	33.5±12.0	33.4±23.3	0.785	33.0±20.4	32.4±11.0	33.6±26.5	0.581
LVEF, %	64.0±8.5	63.6±7.5	0.486	64.0±7.6	64.3±7.5	63.6±7.6	0.263
E/E′	10.7±5.2	9.8±5.0	0.011	10.0±4.3	10.0±4.2	9.9±4.4	0.109
LVEDD, mm	49.2±4.3	49.9±4.3	0.022	49.8±4.3	49.3±4.2	49.9±4.3	0.089
Follow-up period, mo	40.8±20.9	41.5±27.6	0.723	40.5±24.4	40.8±20.7	40.1±27.6	0.714

Values are expressed as a n (%) or mean±SD. Chronic kidney disease was defined as an estimated glomerular filtration rate <60 mL/min/1.73 m^2. AF indicates atrial fibrillation; CPVI, circumferential pulmonary vein isolation; E/E′, the ratio of mitral peak velocity of early filling (E) to early diastolic mitral annular velocity (E′); LA, left atrium; LVEDD, left ventricular end-diastolic dimension; LVEF, left ventricular ejection fraction; PS, propensity score; SVC-L, linear ablation from the superior vena cava to the right atrial septum; TIA, transient ischemic attack.

control AAD-resistant recurring atrial arrhythmias (*P*=0.066). At the last follow-up, sinus rhythm was maintained in 96.7% of the SVC-L group (27.9% [83/297] under AADs) and 91.2% of the CPVI group (33.6% [94/280] under AADs) after a single procedure (*P*=0.004). In the multivariate Cox regression analysis, SVC-L in addition to CPVI was independently associated with lower risk of an AF recurrence (hazard ratio: 0.59 [95% CI, 0.44–0.78]; *P*<0.001; Table 3).

In subgroup analyses, the superiority of the rhythm outcome in the SVC-L group was consistent regardless of age, AF type, comorbid factors, and LA size, but it was more significant in male participants (*P*=0.022 for interaction) and those with a prior history of a stroke or transient ischemic attack (*P*=0.017 for interaction) compared with their counterparts (Figure S2).

Change in HRV Parameters After Catheter Ablation

Figure 3 shows changes in the HRV parameters before and at 3 months, 1 year, and 2 years after ablation and compares those parameters between the SVC-L and CPVI groups. Although there was no significant difference in the mean heart rate and HRV parameters for 2 years after CPVI alone, the mean heart rates were significantly higher and the HRV parameters reflecting sympathetic nervous activity (standard deviation of all NN intervals, root mean square of successive differences, or HF) and parasympathetic nervous activity (LF or LF/HF) were significantly reduced for up to 2 years after SVC-L with CPVI. The HRV differences between groups were most prominent after 3 months but showed a tendency to return to the baseline level over time. In 2-year HRV, only the mean heart rate (*P*=0.018), LF (*P*=0.018), and LF/HF (*P*=0.011) continued to have significant differences between the SVC-L and CPVI groups (Table S1). The postablation changes in mean heart rate and HRV parameters remained significantly for more than 2 years in SVC-L patients without a recurrence than in those with a recurrence or in the CPVI group (Figure S3).

Computer Simulation Study Results

We conducted a computational modeling study integrated with 10 AF patients' cardiac imaging (Table S2), and

Table 2. Comparison of Procedural Results and Clinical Outcomes

	PS-Matched (1:1) Population			
	Overall After PS Match (n=614)	SVC-L Group (n=307)	CPVI Group (n=307)	*P* Value
Procedure time, min	175±41	184±34	165±44	<0.001
Ablation time, s	4817±1047	4809±1046	3996±1220	<0.001
Major complications	12 (2.0)	7 (2.3)	5 (1.6)	0.560
Pericardial effusion	11 (1.8)	6 (2.0)	5 (1.6)	
Phrenic nerve palsy	0 (0.0)	0 (0.0)	0 (0.0)	
Atrioventricular block	1 (0.2)	1 (0.3)	0 (0.0)	
Clinical outcomes				
Follow-up period, mo	40.5±24.4	40.8±20.7	40.1±27.6	0.714
Early recurrence	175 (28.5)	75 (24.4)	100 (32.6)	0.025
Clinical recurrence	222 (36.2)	80 (26.1)	142 (46.3)	<0.001
Recurrence as AF, n (%)	153 (68.9)	57 (71.3)	96 (67.6)	0.573
Recurrence as AT, n (%)	69 (31.1)	23 (28.7)	46 (32.4)	0.573
Cardioversion, n (%)	38 (17.1)	13 (16.3)	25 (17.6)	0.797
Remained in SR without AADs, n (%)	400 (65.1)	214 (69.7)	186 (60.6)	0.018
Final rhythm in sinus, n (%)	577 (94.0)	297 (96.7)	280 (91.2)	0.004
Drug use after ablation				
AADs at discharge, n (%)	34 (5.5)	17 (5.5)	17 (5.5)	1.000
AADs after 3 mo, n (%)	114 (18.6)	47 (15.3)	67 (21.8)	0.038
AADs at final follow-up, n (%)	191 (31.1)	89 (29.0)	102 (33.2)	0.257
β-Blocker, n (%)	201 (32.7)	99 (32.2)	102 (33.2)	0.796

AAD indicates antiarrhythmic drug; AF indicates atrial fibrillation; AT, atrial tachycardia; CPVI, circumferential pulmonary vein isolation; PS, propensity score; SR, sinus rhythm; SVC-L, linear ablation from the superior vena cava to the right atrial septum.

compared the virtual ablation protocols of CPVI alone and CPVI and SVC-L (30 episodes; Table S3). AF termination and defragmentation rates increased after the additional SVC-L protocol compared with CPVI alone (100% versus 50%, *P*=0.033). Ablation in the SVC-L group reduced dominant frequency values significantly more than in the

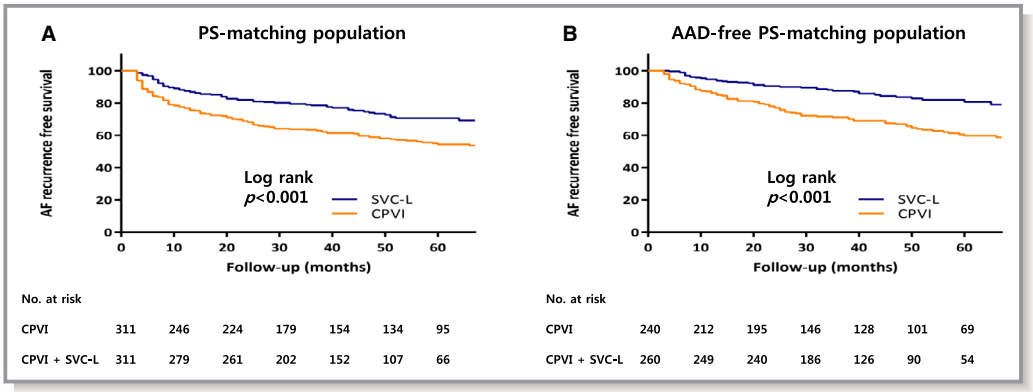

Figure 2. Kaplan–Meier curves for AF recurrence-free survival rate (**A**) and AF and AAD-free survival rate (**B**) according to the ablation strategies in PS-matched population. AAD indicates antiarrhythmic drug; AF, atrial fibrillation; CPVI, circumferential pulmonary vein isolation; PS, propensity score; SVC-L, linear ablation from the superior vena cava to the right atrial septum.

Table 3. Cox Regression Analysis for the Prediction of AF Recurrence After Ablation

	PS-Matched (1:1) Population			
	Univariable		Multivariable	
	HR (95% CI)	*P* Value	HR (95% CI)	*P* Value
Age	1.000 (0.988–1.012)	0.990	0.998 (0.985–1.010)	0.704
Male	0.775 (0.583–1.029)	0.078	0.720 (0.538–0.964)	0.027
Persistent AF	1.158 (0.813–1.651)	0.416	1.087 (0.748–1.578)	0.663
Heart failure	1.406 (0.832–2.377)	0.203	. . .	. . .
Hypertension	1.188 (0.910–1.551)	0.205	. . .	. . .
Diabetes mellitus	1.085 (0.710–1.659)	0.705	. . .	. . .
Prior stroke/TIA	1.464 (0.950–2.256)	0.084	. . .	. . .
Chronic kidney disease	1.468 (0.960–2.244)	0.077	. . .	. . .
CHA_2DS_2-VASc score	1.091 (0.994–1.199)	0.068	. . .	. . .
Echocardiography				
LA dimension, mm	1.045 (1.021–1.069)	<0.001	1.044 (1.020–1.068)	<0.001
LA volume index, mL/m^2	1.009 (1.005–1.013)	<0.001	. . .	. . .
LVEF, %	0.986 (0.970–1.002)	0.085	. . .	. . .
E/E′	1.007 (0.982–1.032)	0.586	. . .	. . .
HRV				
Mean heart rate, beats/min	1.001 (0.990–1.013)	0.852	. . .	. . .
SDNN, ms	1.001 (0.997–1.006)	0.503	. . .	. . .
rMSSD, ms	1.009 (0.998–1.021)	0.117	. . .	. . .
LF, Hz	0.999 (0.993–1.004)	0.647	. . .	. . .
HF, Hz	1.013 (0.988–1.038)	0.312	. . .	. . .
LF/HF ratio	0.885 (0.611–1.282)	0.518	. . .	. . .
Ablation group				
CPVI+SVC-L	0.567 (0.431–0.747)	<0.001	0.586 (0.442–0.777)	<0.001

A multivariable model was adjusted for age, sex, type of AF, LA dimension on echocardiogram, and ablation strategy. These covariates were selected on the basis of their previously established role as predictive factors for recurrence of AF. AF indicates atrial fibrillation; CPVI, circumferential pulmonary vein isolation; HF, high-frequency components; HR, hazard ratio; HRV, heart rate variability; LA, left atrium; LF, low-frequency components; LVEF, left ventricular ejection fraction; PS, propensity score; rMSSD, root mean square of the successive differences; SDNN, standard deviation of all NN intervals; SVC-L, linear ablation from the superior vena cava to the right atrial septum; TIA, transient ischemic attack.

CPVI group (4.40±0.72 versus 4.76±0.13 Hz, $P<0.001$; Figure S4).

Discussion

Main Findings

In this study, we found that long-term rhythm outcomes over 2 years were significantly better after SVC-L in addition to CPVI than after CPVI alone, without increasing the complication rate. The potential mechanisms of SVC-L seem to affect the cardiac ANS and AF wave dynamics. In the HRV analysis performed during the second year, the mean hazard ratio was higher and HRV attenuation persisted in the SVC-L group compared with the CPVI group. In the simulation modeling study, we observed a significant reduction in dominant frequency and an increased AF termination rate after SVC-L.

Role of the ANS in AF

More than 14 000 autonomic neurons are distributed in the heart. The cardiac ANS can be divided into the extrinsic cardiac ANS and the intrinsic cardiac ANS.[5] The extrinsic cardiac ANS has stellate ganglia (C7-T2) as the gateway of sympathetic innervation, and most extrinsic vagal nerve fibers gather in the third fat pad (gatekeeper ganglia) located between the SVC and the aorta.[10] With the complex neural networking among the cardiac ANS, the sympathovagal coactivation of PV sites has been shown to induce paroxysmal AF,[15,16] and autonomic remodeling contributes to AF

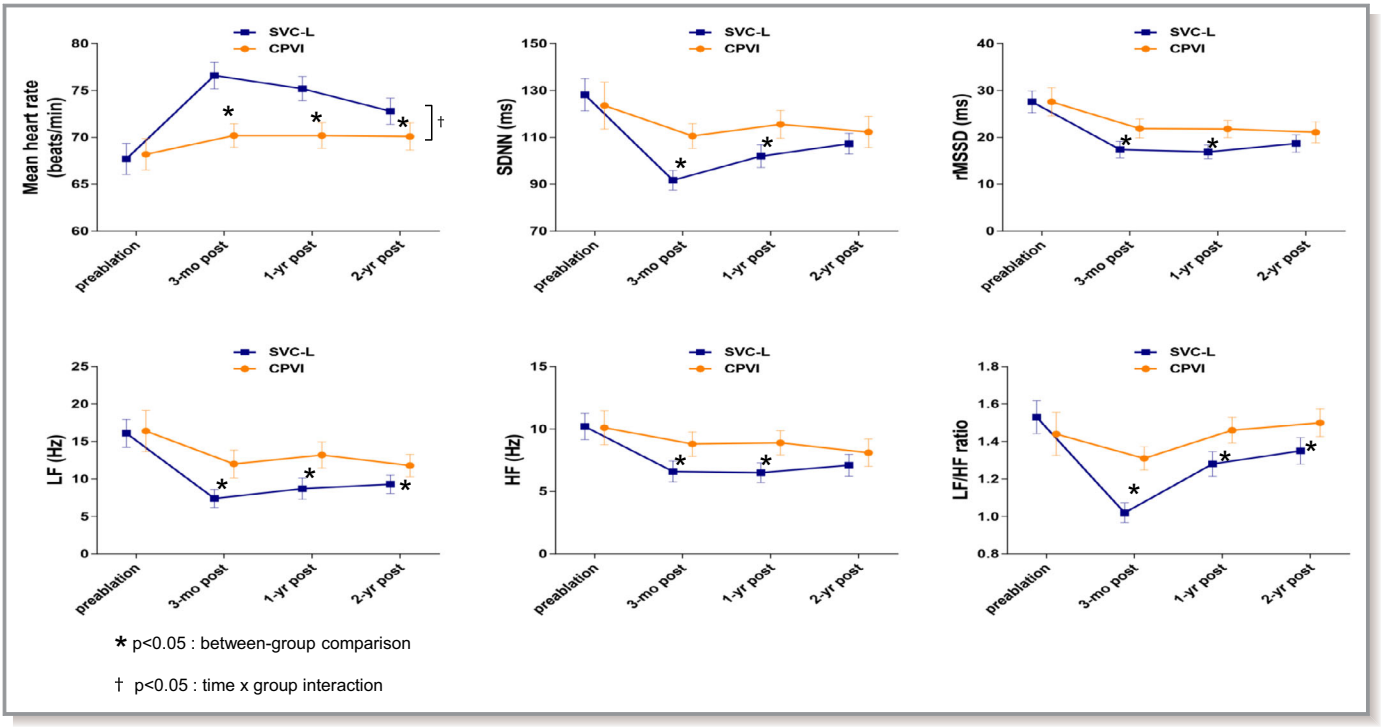

Figure 3. Changes in mean heart rate and heart rate variability parameters depending on the ablation strategies before and 3 months, 1 year, and 2 years after ablation. CPVI indicates circumferential pulmonary vein isolation; HF, high-frequency components; LF, low-frequency components; rMSSD, root mean square of the successive differences; SDNN, standard deviation of all NN intervals; SVC-L, linear ablation from the superior vena cava to the right atrial septum.

substrate formation.[17,18] The cardiac ANS plays an important role in triggering and maintaining arrhythmias, mainly when the sympathovagal balance is shaken.[2–4] Strong sympathetic stimulation induces atrial and ventricular arrhythmias via unopposed sympathetic stimulation by delaying the vagal output in cholinergic ganglia by promoting the release of neuropeptide Y or galanin.[2–4] Conversely, sustained vagal activation stimulates α-7 nicotinic anti-inflammatory pathway and causes antiapoptotic effects.[2–4] In GPs, the cellular calcium release by sympathetic neural activation and a shortening of action potential duration by parasympathetic neural activation generate phase 3 early after depolarization conditions, which are known to contribute to PV triggering and AF induction.[19–22]

Cardiac ANS Effects of SVC-L

Various cardiac ANS modulations have been introduced for cardiac arrhythmia suppression. To suppress atrial arrhythmias, low-level vagus nerve stimulation at the tragus[23] or renal sympathetic denervation[24] have been introduced. However, the most commonly used cardiac neuromodulation is CPVI during the AF ablation procedure. This is because GPs are located within 5 mm of the LA–PV junction.[25] Pappone et al[7] reported, for the first time, that the recurrence rate was low in patients with 3-month HRV attenuation after CPVI. Katritsis et al[8] reported a 48% success rate with selective GP ablation alone but achieved better results with combined CPVI and GP ablation. Although the majority of included patients had nonparoxysmal AF, the AFACT (Atrial Fibrillation Ablation and Autonomic Modulation via Thoracoscopic Surgery) trial reported that additional GP ablation during thoracoscopic AF surgery did not benefit the rhythm outcome.[9]

Kang et al[11] named the SVC-L, a linear ablation from the highest point with the SVC potentials at the septal aspect to the posterior superior limbus of the fossa ovalis. Although SVC-L does not ablate the entire third fat pad, it appears to cross and ablate the cardiac nerve branches from the third fat pad and superior right GP area with cardiac ANS-modulating effects.[11,12,26] Debruyne et al[12] also reported a therapeutic effect in patients with neurally mediated syncope and functional sinus node dysfunction by focal ablation of the anterior right GP area from an RA septal site, which is included in the SVC-L. In this study, an extrinsic cardiac ANS modulation effect was maintained for >2 years, and the mean heart rate, LF, and LF/HF ratio continued to have significant differences between the SVC-L and CPVI groups. It is hard to differentiate the changes in extrinsic or intrinsic cardiac ANS and sympathetic or parasympathetic nerves,[5,6] and tissue injury can regenerate intrinsic cardiac nerves.[27]

However, the effect of SVC-L was not significant in patients with persistent AF.

Changes in Wave Dynamics After SVC-L

We speculate about another potential effect of SVC-L in terms of changing wave dynamics. SVC-L may reduce AF recurrence by creating radiofrequency lesions on the RA posterior septal wall, where HCN4 (hyperpolarization activated cyclic nucleotide gated potassium channel 4)–positive cells with automaticity[28] and nonuniform anisotropy exist. SVC-L is in contact with the right side of the PV antral ablation line on the RA side, which might cut the unstable reentry circuit including the right- and left-sided high septum and Bachmann's bundle.[11] Based on these various mechanisms, this study demonstrated in a simulation modeling study that SVC-L has antifibrillatory effects that lower the dominant frequency value reflecting the AF driver and increase the AF termination or defragmentation rate.

Potential Complications and Limitations

Although transient sinus node dysfunction occurred after SVC-L in a few patients, the ablation site was clearly away from the sinus node and all affected patients recovered spontaneously within 24 hours. Myocardial damage associated with SVC-L may promote the secretion of neurotrophic factors and nerve sprouting,[29] and the resulting heterogeneous reinnervation of the cardiac ANS can produce proarrhythmic conditions.[27] SVC-L is limited in that there is no clear end point to identify the bidirectional block, but sufficient radiofrequency lesion formation can be proven by comparing the voltage maps before and after SVC-L.[11] This study included a highly selective group of patients who were referred for catheter ablation, and the number of patients was also limited. Although we conducted propensity score matching, the operator's preference for additional SVC-L cannot be excluded. However, the timing for both groups did not differ (40.8±20.9 versus 41.5±27.6 months, P=0.723), and the improvement in mapping and ablation technology did not affect the comparison outcome.

Conclusions

SVC-L in addition to CPVI significantly improved long-term rhythm outcome over 2 years after AF catheter ablation by mechanisms involving autonomic modulation and AF organization.

Acknowledgments

We would like to thank John Martin for his linguistic assistance.

Sources of Funding

This work was supported by grants (HI18C0070 and HI19C0114) from the Ministry of Health and Welfare and a grant (NRF-2017R1A2B4003983 and NRF-2019R1C1C1009075) from the Basic Science Research Program of the National Research Foundation of Korea, which is funded by the Ministry of Science, ICT (information and communications technology), and Future Planning.

Disclosures

None.

References

1. Coumel P, Attuel P, Lavallee J, Flammang D, Leclercq JF, Slama R. [The atrial arrhythmia syndrome of vagal origin]. *Arch Mal Coeur Vaiss*. 1978;71:645–656.
2. Brack KE, Coote JH, Ng GA. Vagus nerve stimulation protects against ventricular fibrillation independent of muscarinic receptor activation. *Cardiovasc Res*. 2011;91:437–446.
3. Calvillo L, Vanoli E, Andreoli E, Besana A, Omodeo E, Gnecchi M, Zerbi P, Vago G, Busca G, Schwartz PJ. Vagal stimulation, through its nicotinic action, limits infarct size and the inflammatory response to myocardial ischemia and reperfusion. *J Cardiovasc Pharmacol*. 2011;58:500–507.
4. Herring N, Cranley J, Lokale MN, Li D, Shanks J, Alston EN, Girard BM, Carter E, Parsons RL, Habecker BA, Paterson DJ. The cardiac sympathetic co-transmitter galanin reduces acetylcholine release and vagal bradycardia: implications for neural control of cardiac excitability. *J Mol Cell Cardiol*. 2012;52:667–676.
5. Armour JA, Murphy DA, Yuan BX, Macdonald S, Hopkins DA. Gross and microscopic anatomy of the human intrinsic cardiac nervous system. *Anat Rec*. 1997;247:289–298.
6. Kawashima T. The autonomic nervous system of the human heart with special reference to its origin, course, and peripheral distribution. *Anat Embryol (Berl)*. 2005;209:425–438.
7. Pappone C, Oral H, Santinelli V, Vicedomini G, Lang CC, Manguso F, Torracca L, Benussi S, Alfieri O, Hong R, Lau W, Hirata K, Shikuma N, Hall B, Morady F. Atrio-esophageal fistula as a complication of percutaneous transcatheter ablation of atrial fibrillation. *Circulation*. 2004;109:2724–2726.
8. Katritsis DG, Pokushalov E, Romanov A, Giazitzoglou E, Siontis GC, Po SS, Camm AJ, Ioannidis JP. Autonomic denervation added to pulmonary vein isolation for paroxysmal atrial fibrillation: a randomized clinical trial. *J Am Coll Cardiol*. 2013;62:2318–2325.
9. Driessen AHG, Berger WR, Krul SPJ, van den Berg NWE, Neefs J, Piersma FR, Chan Pin Yin D, de Jong J, van Boven WP, de Groot JR. Ganglion plexus ablation in advanced atrial fibrillation: the AFACT study. *J Am Coll Cardiol*. 2016;68:1155–1165.
10. Chiou CW, Eble JN, Zipes DP. Efferent vagal innervation of the canine atria and sinus and atrioventricular nodes. The third fat pad. *Circulation*. 1997;95:2573–2584.
11. Kang KW, Pak HN, Park J, Park JG, Uhm JS, Joung B, Lee MH, Hwang C. Additional linear ablation from the superior vena cava to right atrial septum after pulmonary vein isolation improves the clinical outcome in patients with paroxysmal atrial fibrillation: prospective randomized study. *Europace*. 2014;16:1738–1745.
12. Debruyne P, Rossenbacker T, Collienne C, Roosen J, Ector B, Janssens L, Charlier F, Vankelecom B, Dewilde W, Wijns W. Unifocal right-sided ablation treatment for neurally mediated syncope and functional sinus node dysfunction under computed tomographic guidance. *Circ Arrhythm Electrophysiol*. 2018;11:e006604.
13. Lim B, Hwang M, Song JS, Ryu AJ, Joung B, Shim EB, Ryu H, Pak HN. Effectiveness of atrial fibrillation rotor ablation is dependent on conduction velocity: an in-silico 3-dimensional modeling study. *PLoS One*. 2017;12:e0190398.
14. Courtemanche M, Ramirez RJ, Nattel S. Ionic mechanisms underlying human atrial action potential properties: insights from a mathematical model. *Am J Physiol*. 1998;275:H301–H321.

15. Patterson E, Po SS, Scherlag BJ, Lazzara R. Triggered firing in pulmonary veins initiated by in vitro autonomic nerve stimulation. *Heart Rhythm*. 2005;2:624–631.
16. Bettoni M, Zimmermann M. Autonomic tone variations before the onset of paroxysmal atrial fibrillation. *Circulation*. 2002;105:2753–2759.
17. Ng J, Villuendas R, Cokic I, Schliamser JE, Gordon D, Koduri H, Benefield B, Simon J, Murthy SN, Lomasney JW, Wasserstrom JA, Goldberger JJ, Aistrup GL, Arora R. Autonomic remodeling in the left atrium and pulmonary veins in heart failure: creation of a dynamic substrate for atrial fibrillation. *Circ Arrhythm Electrophysiol*. 2011;4:388–396.
18. Yu L, Scherlag BJ, Sha Y, Li S, Sharma T, Nakagawa H, Jackman WM, Lazzara R, Jiang H, Po SS. Interactions between atrial electrical remodeling and autonomic remodeling: how to break the vicious cycle. *Heart Rhythm*. 2012;9:804–809.
19. Chen PS, Chen LS, Fishbein MC, Lin SF, Nattel S. Role of the autonomic nervous system in atrial fibrillation: pathophysiology and therapy. *Circ Res*. 2014;114:1500–1515.
20. Burashnikov A, Antzelevitch C. Reinduction of atrial fibrillation immediately after termination of the arrhythmia is mediated by late phase 3 early afterdepolarization-induced triggered activity. *Circulation*. 2003;107:2355–2360.
21. Patterson E, Jackman WM, Beckman KJ, Lazzara R, Lockwood D, Scherlag BJ, Wu R, Po S. Spontaneous pulmonary vein firing in man: relationship to tachycardia-pause early afterdepolarizations and triggered arrhythmia in canine pulmonary veins in vitro. *J Cardiovasc Electrophysiol*. 2007;18:1067–1075.
22. Hwang M, Lim B, Song JS, Yu HT, Ryu AJ, Lee YS, Joung B, Shim EB, Pak HN. Ganglionated plexi stimulation induces pulmonary vein triggers and promotes atrial arrhythmogenecity: in silico modeling study. *PLoS One*. 2017;12:e0172931.
23. Yu L, Scherlag BJ, Li S, Fan Y, Dyer J, Male S, Varma V, Sha Y, Stavrakis S, Po SS. Low-level transcutaneous electrical stimulation of the auricular branch of the vagus nerve: a noninvasive approach to treat the initial phase of atrial fibrillation. *Heart Rhythm*. 2013;10:428–435.
24. Linz D, Mahfoud F, Schotten U, Ukena C, Neuberger HR, Wirth K, Bohm M. Renal sympathetic denervation suppresses postapneic blood pressure rises and atrial fibrillation in a model for sleep apnea. *Hypertension*. 2012;60:172–178.
25. Tan AY, Li H, Wachsmann-Hogiu S, Chen LS, Chen PS, Fishbein MC. Autonomic innervation and segmental muscular disconnections at the human pulmonary vein-atrial junction: implications for catheter ablation of atrial-pulmonary vein junction. *J Am Coll Cardiol*. 2006;48:132–143.
26. Kang KW, Kim TH, Park J, Uhm JS, Joung B, Hwang C, Lee MH, Pak HN. Long-term changes in heart rate variability after radiofrequency catheter ablation for atrial fibrillation: 1-year follow-up study with irrigation tip catheter. *J Cardiovasc Electrophysiol*. 2014;25:693–700.
27. Mao J, Yin X, Zhang Y, Yan Q, Dong J, Ma C, Liu X. Ablation of epicardial ganglionated plexi increases atrial vulnerability to arrhythmias in dogs. *Circ Arrhythm Electrophysiol*. 2014;7:711–717.
28. Yamamoto M, Dobrzynski H, Tellez J, Niwa R, Billeter R, Honjo H, Kodama I, Boyett MR. Extended atrial conduction system characterised by the expression of the HCN4 channel and connexin45. *Cardiovasc Res*. 2006;72:271–281.
29. Okuyama Y, Pak HN, Miyauchi Y, Liu YB, Chou CC, Hayashi H, Fu KJ, Kerwin WF, Kar S, Hata C, Karagueuzian HS, Fishbein MC, Chen PS, Chen LS. Nerve sprouting induced by radiofrequency catheter ablation in dogs. *Heart Rhythm*. 2004;1:712–717.

Supplemental Material

Table S1. **Comparison of the HRV parameters depending on the ablation strategy in the propensity score-matched population.**

	CPVI (n=307)	**SVC-L (n=307)**	P value
HRV preablation			
Mean heart rate (BPM)	68.2±13.2	67.7 ± 12.3	0.705
SDNN (ms)	123.6±61.7	128.2 ± 45.4	0.427
rMSSD (ms)	27.6±18.4	27.6 ± 15.5	0.994
LF (Hz)	16.4±17.1	16.1 ± 12.4	0.821
HF (Hz)	10.1±8.4	10.2 ± 6.9	0.868
LF/HF ratio	1.44±0.70	1.53 ± 0.58	0.173
HRV 3months			
Mean heart rate (BPM)	70.2±10.5	76.6 ± 11.4	<0.001
SDNN (ms)	110.6±42.6	91.7 ± 33.2	<0.001
rMSSD (ms)	21.9±16.2	17.4 ± 14.0	0.001
LF (Hz)	12.0±15.1	7.4 ± 9.5	<0.001
HF (Hz)	8.8±7.9	6.6 ± 6.6	0.001
LF/HF ratio	1.31±0.50	1.02 ± 0.42	<0.001
HRV 1year			
Mean heart rate (BPM)	70.2±10.4	75.2 ± 10.2	<0.001
SDNN (ms)	115.6±44.4	102.0 ± 38.3	<0.001
rMSSD (ms)	21.8±13.6	16.9 ± 11.4	<0.001
LF (Hz)	13.2±13.0	8.7 ± 11.0	<0.001
HF (Hz)	8.9 ± 7.2	6.5 ± 6.2	<0.001
LF/HF ratio	1.46±0.51	1.28 ± 0.51	<0.001
HRV 2year			
Mean heart rate (BPM)	70.1±9.8	72.8 ± 10.2	0.018
SDNN (ms)	112.3±42.0	107.3 ± 32.1	0.230
rMSSD (ms)	21.1±14.0	18.7 ± 13.5	0.132
LF (Hz)	11.8±9.8	9.3 ± 8.9	0.018
HF (Hz)	8.1±7.3	7.1 ± 6.3	0.188
LF/HF ratio	1.50±0.50	1.35 ± 0.51	0.011

HF: high frequency, HRV: heart rate variability, LF: low frequency, rMSSD: root mean square of the successive differences, SDNN: standard deviation of all NN intervals.

Table S2. **Patient characteristics of the computer simulation study (10 patients).**

Age	64.9 ± 10.1
Male (%)	9 (90)
CHA_2DS_2-VASc score	1.30 ± 1.27
Paroxysmal AF (%)	10 (100)
Heart failure (%)	1 (10)
Hypertension (%)	4 (40)
Diabetes (%)	1 (10)
Previous stroke (%)	0 (0)
Previous TIA (%)	0 (0)
Vascular disease (%)	0 (0)
LA dimension (mm)	39.6 ± 5.5
LVEF	62.0 ± 18.5
E/E’	9.2 ± 4.6

TIA: transient ischemic attack, LVEF: left ventricular ejection fraction, E/E’: the ratio of mitral peak velocity of early filling (E) to early diastolic mitral annular velocity (E')

Table S3. **Virtual ablation outcome in 10 patients.**

Ablation protocol	Number of episodes	AF maintenance	AF termination	AF termination or change to AT
Baseline	10	50% (5/10)	20% (2/10)	50% (5/10)
CPVI alone	10	50% (5/10)	30% (3/10)	50% (5/10)
CPVI + SVC-L	10	0% (0/10)*	40% (4/10)	100% (10/10)*

* p=0.033 vs. Baseline or CPVI alone. The AF termination rate was determined within 60s after the virtual intervention. CPVI: circumferential pulmonary vein isolation, SVC-L: superior vena cava to right atrial septum linear ablation.

Figure S1. An SVC-L ablation shown in fluoroscopic views (A and B) and a 3D electroanatomical map (C and D). E. Bipolar electrograms before and after SVC-L ablation. Numbers represent the locations where the electrograms were recorded.

Ds: distal electrode, Px: proximal electrode, SVC-L: superior vena cava to right atrial septum linear ablation.

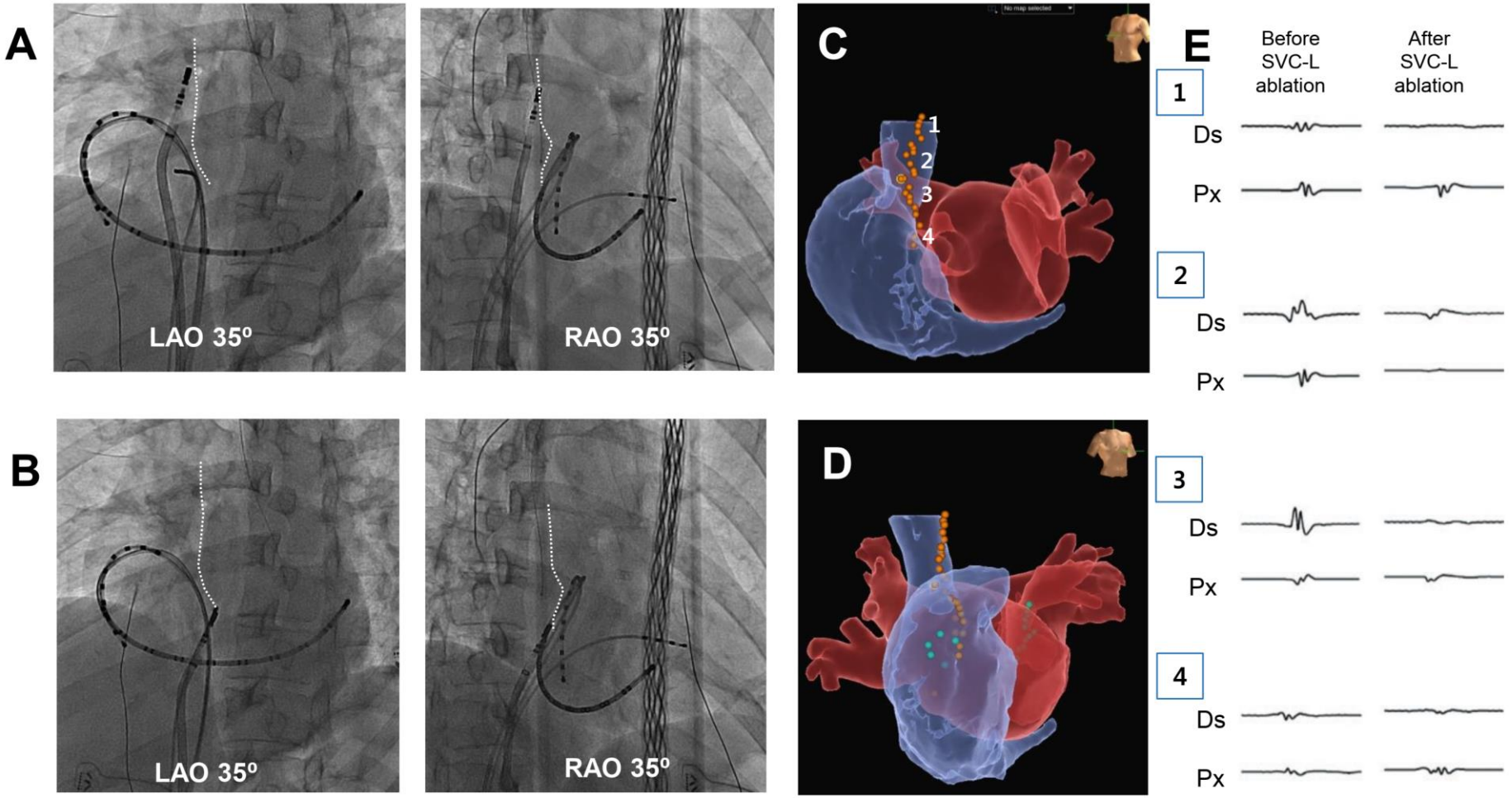

Figure S2. Forest plot displaying the hazard ratio for AF recurrence of the SVC-L compared with CPVI alone among various subgroups. AF: atrial fibrillation, CPVI: circumferential pulmonary vein isolation, SVC-L: superior vena cava to right atrial septum linear ablation.

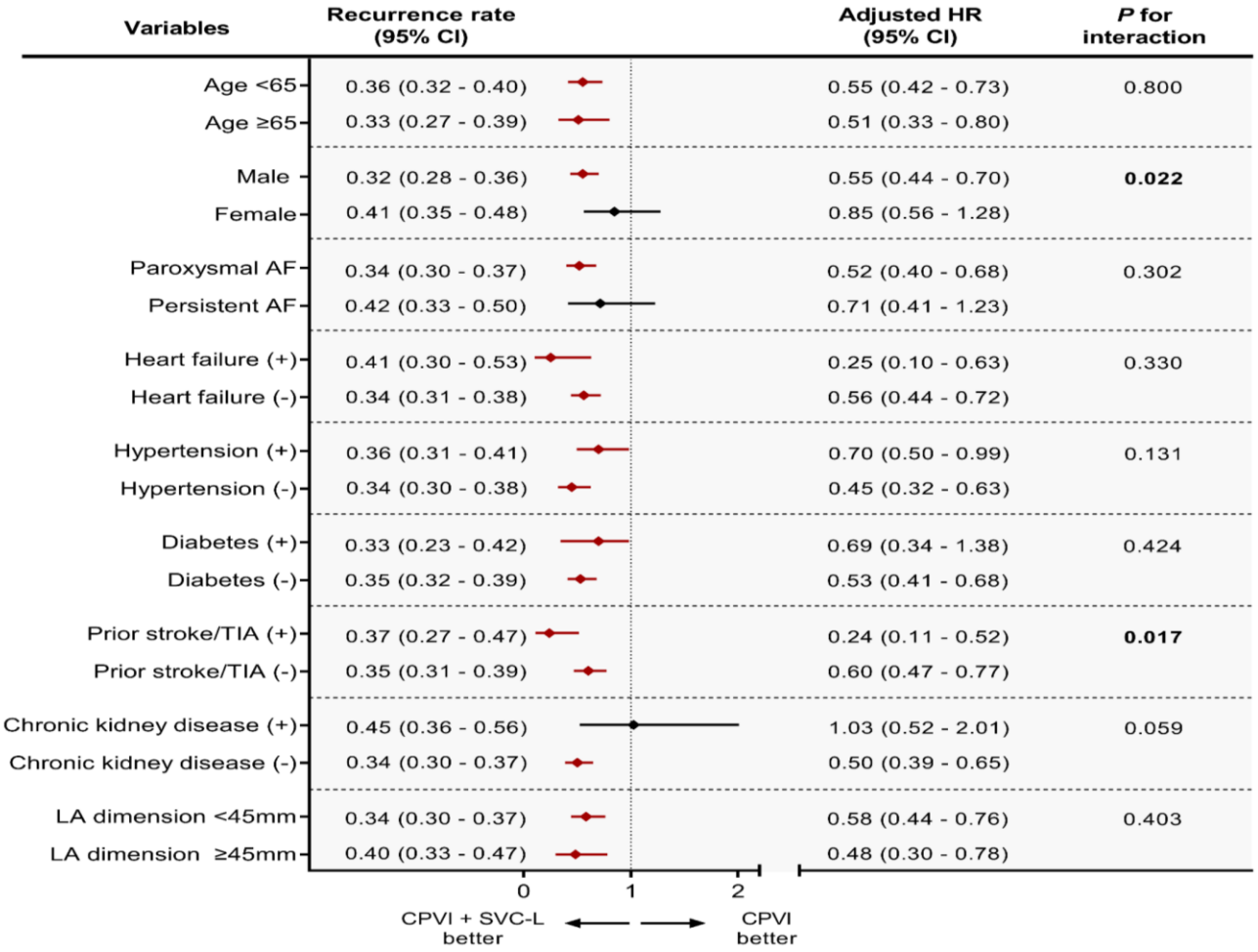

Figure S3. Change of heart rate variability parameters according to the rhythm outcomes of ablation strategy. CPVI: circumferential pulmonary vein isolation alone group, SVC-L: circumferential pulmonary vein isolation plus superior vena cava to right atrial septum linear ablation group.

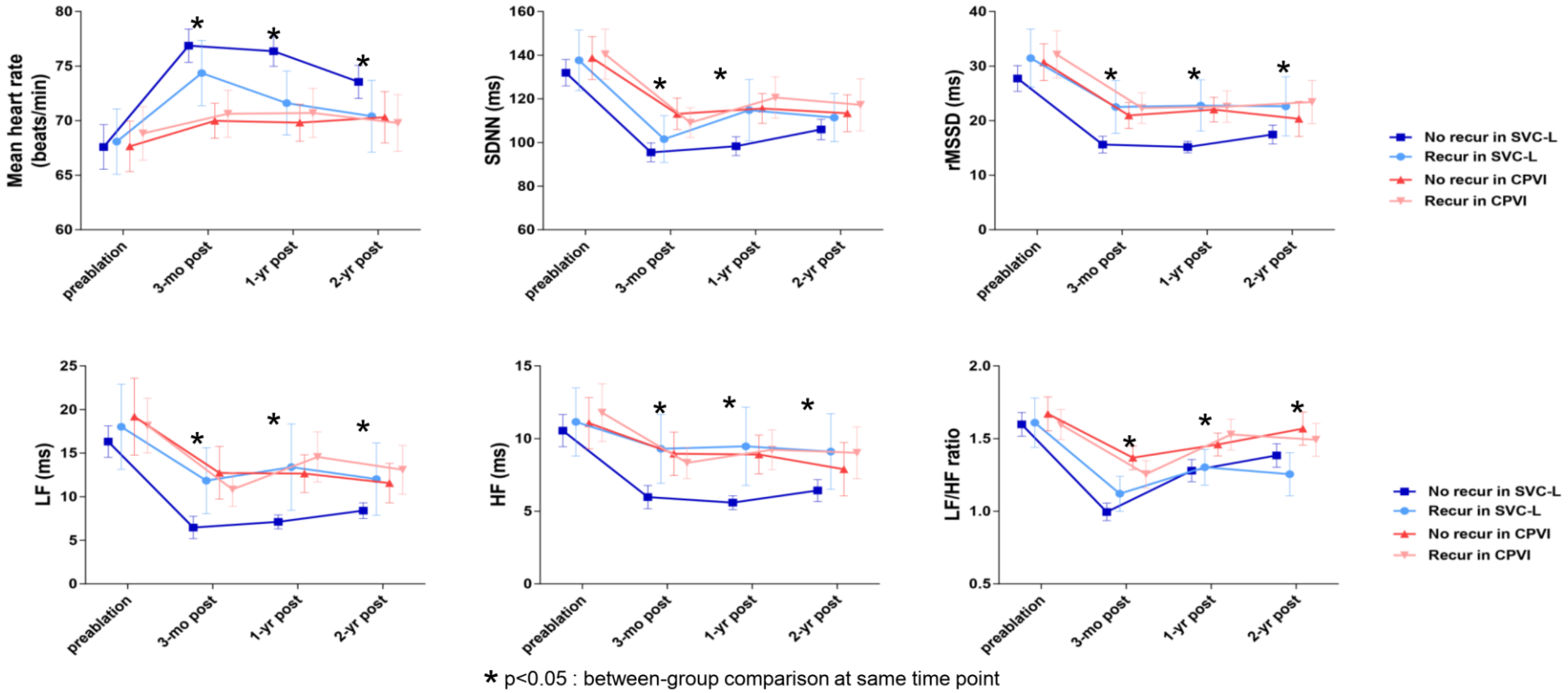

Figure S4. Computational modeling outcome of virtual AF ablation in bi-atrial simulation model. A. Baseline AF sustaining longer than 60 sec. B. After CPVI alone, AF maintained, but changed to organized pattern. C. After SVC-L ablation in addition to CPVI, AF terminated at 49 sec. Left-side color map represents color-coded dominant frequency map. Virtual ablation sites are marked by green line on the right-side white map. Electrogram strips on the bottom represent action potential recording at the high septal area. D. Changes of mean DF values before and after virtual interventions. AF: atrial fibrillation, CPVI: circumferential pulmonary vein isolation, DF: dominant frequency, SVC-L: superior vena cava to right atrial septum linear ablation.